International Journal of Multiphase Flow 35 (2009) 1119–1129

Contents lists available at ScienceDirect

International Journal of Multiphase Flow

journal homepage: www.elsevier.com/locate/ijmulflow

Jump conditions for filtered quantities at an under-resolved discontinuous interface. Part 2: *A priori* tests

A. Toutant [a,b,c,*], M. Chandesris [a], D. Jamet [a], O. Lebaigue [a]

[a] CEA, DEN, DER/SSTH/LMDL, F-38054 Grenoble, France
[b] PROMES-CNRS, UPR 8521, Perpignan, France
[c] Université de Perpignan Via Domitia, France

ARTICLE INFO

Article history:
Received 28 November 2008
Received in revised form 29 May 2009
Accepted 22 July 2009
Available online 23 August 2009

Keywords:
Two-phase flow
Jump conditions
Matched asymptotic expansions
Filter
Surface tension
Turbulence
DNS
LES
Scale similarity hypothesis
Curvature
Front-Tracking method

ABSTRACT

In order to study and validate the jump conditions established in part 1, we realize *a priori* tests thanks to the data of a 3D Direct Numerical Simulation (DNS) of a strongly deformable bubble in a spatially decaying turbulence. The complex interactions between interface and turbulence are fully resolved. An explicit filtering of the DNS has been employed to evaluate the filtered quantities and to check the potential of the models for two-phase flows in the Interface and Subgrid Scales (ISS) modeling case proposed in part 1. The ISS concept is our proposal of a two-phase equivalent for the one-phase Large Eddy Simulation (LES) modeling case with sharp-interfaces. In this concept, bubbles remain bigger than the mesh size. Due to the impossibility to define a filter equivalent to the matched asymptotic expansions, we only test the modeling of the equivalent interface transport (the momentum jump conditions are not tested in this article, but will deserve additional results in *a posteriori* tests). Because the closure of the transport equation of the under-resolved discontinuous interface requires more modeling assumptions than the closure of the momentum equation, we think that the most relevant test has been done. The *a priori* tests realized show excellent agreement between the ISS models and the real contributions.

1. Introduction

The prediction of bubbly turbulent flows is a problem of considerable importance in a variety of applications such as convective boiling, spray formation and direct contact heat exchanger. Because these flows are characterized by the presence of a great number of scales, it is impossible to use Direct Numerical Simulation (DNS) for industrial applications. A promising tool would be an equivalent of Large Eddy Simulation (LES) for two-phase flows.

In part 1 (Toutant et al., accepted for publication), we propose the Interface and Subgrid Scales (ISS) concept. Like the single-phase LES concept, it consists in solving the two-phase flow features at the grid scale of the numerical method and to take into account the unresolved scales with subgrid models. However, we restrict the model in that the filter is much smaller than the bubbles. In this paper, we realize a DNS to make *a priori* tests of the ISS concept. Indeed, the DNS data allow to estimate both the real subgrid terms and the ISS model subgrid terms. Thus, we can compare the real and the ISS terms and evaluate the model.

Because it is impossible to define a filter equivalent to the matched asymptotic expansions, we only test the modeling of the equivalent interface transport.[1] Indeed, it is easier to test the interface transport than the momentum equation. This is due to the fact that the interface transport only requires the velocity at the interface and the momentum equation the velocity gradient at the interface. Fortunately, the test of the interface transport is more relevant than the test of the momentum equation because more closure assumptions have been done for the interface transport than for the momentum equation. The differences between the closures of these two equations are explained in the next paragraph.

To find the ISS closures, we have used three levels of description: DNS, continuous LES and discontinuous LES. Two up-scaling steps correspond to these three levels. This paper is dedicated to the validation of the second up-scaling step (from continuous to discontinuous LES). The first up-scaling step (from DNS to continuous LES) makes appear one subgrid term in the transport of the

* Corresponding author. Address: CEA, DEN, DER/SSTH/LMDL, F-38054 Grenoble, France.
E-mail address: adrien.toutant@univ-perp.fr (A. Toutant).

[1] The momentum jump conditions are not tested in this article, but will deserve additional results in *a posteriori* tests.

0301-9322/$ - see front matter © 2009 Elsevier Ltd. All rights reserved.
doi:10.1016/j.ijmultiphaseflow.2009.07.010

under-resolved continuous interface and two subgrid terms in the momentum equation. The modeling of these three subgrid terms using a scale similarity hypothesis is validated in Toutant et al. (2008). In this previous work, DNS data are used to realize *a priori* tests. The proposed closures at the continuous LES level are compared to the real contribution of the corresponding subgrid term. The results show that the closures are very well correlated to the real contributions. The second up-scaling step transforms

- the term related to the advection of the momentum equation to the equivalent term for one-phase flow (it is $\tilde{\rho}\widetilde{\mathscr{D}}$ in Eq. (75c) of part 1),
- the term related to the acceleration of the momentum equation to the integral of this term (it is the term III in Eq. (75c) of part 1),
- the term related to the transport of the under-resolved continuous interface to the integral of this term (it is the term I in Eq. (75b) of part 1).

The validity of these transformations depends only on the validity of the assumptions made for applying the method of the matched asymptotic expansions. The choice of the location of the discontinuous interface implies that no more terms appear in the momentum equation. However, another term appears in the equation of the transport of the under-resolved discontinuous interface whatever its location (it is the term II in Eq. (75b) of part 1). Initially, this new term is not closed. Its modeling requires two new assumptions: an approximation of the interface and a particular choice of the kernel filter G. The interface is approximated by a surface whose curvature is linearly varying between the principal curvatures (Eq. (61) part 1 Toutant et al., accepted for publication) and the filter is chosen spherical (Eq. (62) part 1 Toutant et al., accepted for publication). In addition to these two new assumptions, the modeling of the interface transport uses the time evolution of the principal curvature that is also a result of part 1 (see Appendix D of part 1 Toutant et al., accepted for publication). These are the reasons why the tests dedicated to the equation of the transport of the under-resolved discontinuous interface (Eq. (75b) of part 1) are the most relevant tests. We choose to perform *a priori* tests. At each time step, each closure is compared to the real contribution of the corresponding subgrid term. *A priori* tests will allow to know if the proposed closure is structurally very close to the real subgrid term.

In Section 2, we present a relevant DNS of the interaction between a buoyant bubble and a spatially decaying turbulence. In Section 3, we perform with the DNS data *a priori* tests to evaluate the validity of the closures to model the velocity of the under-resolved discontinuous interface (see part 1 Toutant et al., accepted for publication). Conclusions and perspectives are finally drawn.

2. A relevant simulation at the DNS level

In the context of DNS of two-phase flows, most of the literature is dedicated to two types of studies.

- On the one hand, computations focus on deformable interfaces but not really on developed turbulence. For instance, Bunner and Tryggvason (2003) study the effect of bubble deformation on the properties of bubbly flows (Bunner and Tryggvason, 2003). In their simulations, vortical structures are only produced by the wake of bubbles. The so-called pseudo-turbulence induced by a bubble swarm does not have the same properties as a really developed turbulence whose energy spectrum has an inertial zone.
- On the other hand, the turbulence is fully developed but the interfaces are non-deformable. Thus, complex interactions between fluid velocity fluctuations and interface deformations cannot exist. In a large amount of works in this category, the size of the particles is smaller than the Kolmogorov length scale (Février et al., 2005) and, even when the particle's diameter is much larger than this scale, bubbles are supposed to be non-deformable. For example, Merle et al. (2005) simulate the dynamics of a clean spherical bubble fixed in a turbulent pipe flow (Merle et al., 2005).

In addition to these two types of studies, a recent work of Lu et al. (2005) is dedicated to the study of deformable bubbles in turbulent channel flows. This study based on several DNS is very complete, several physical phenomena occur: turbulence production at the wall, effect of the bubble wakes, interaction between the bubbles, coupling between bubbles and turbulence. Concerning bubble deformations, the physical conditions are very similar to ours (three Weber numbers are examined 0.203, 0.270 and 0.405). The Reynolds number of Lu et al. using the friction velocity and the half-height of the channel is equal to 135. The simulations performed by Lu et al. could be used in order to test the ISS closure. In the present contribution, we choose a different geometry. We investigate the DNS of the motion of a strongly deformable bubble in a spatially decaying turbulence. It allows us to use a uniform mesh (helpful to perform *a priori* tests) and to reach a turbulent Reynolds number equal to 480. This turbulent Reynolds number is relatively small but it is slightly bigger than the Reynolds number of Lu et al. Thus, the ratio of the bubble curvature radius over the Kolmogorov length scale is also slightly bigger in our case. In this study, we focus our attention on the coupling between interfaces and turbulence (turbulence production, effect of bubble wakes and interaction between bubbles are not taken into account). It is coherent with our approach. Indeed, the ISS concept is a local and instantaneous model. We do not consider the bubble as an entity that interacts with turbulence. We consider the very local problem of the interaction between a *portion* of the bubble (that can be assimilated to a free-surface) and the coherent turbulent structures near the interface. Consequently, a test case to evaluate ISS model is relevant if the Kolmogorov length scale is much smaller than the bubble diameter and the turbulent structures create large deformation of the interface. The realized test case satisfies these conditions.

2.1. Solved equations

To perform the DNS (see Fig. 1 of part 1), we use a "sharp-interface" version of the Front-Tracking approach that does not resort to usual explicit smoothing functions of the interfaces. Since the interfaces are not smeared, the method can capture more accurately the turbulent transfer between the two phases. It was assessed on many application tests comparing the obtained results with analytical solutions or experimental data (Mathieu, 2004). This original method benefits from the VOF method to impose the mass conservation for the computation of the indicator function and from the level-set method to use a signed distance function. Nevertheless, the interfaces are explicitly described using a Lagrangian mesh, moving on an Eulerian mesh for the flux computation as for the classical Front-Tracking method. The system (1) is approximated by explicit finite volumes of second order in space (the convection operator is centered) and third order in time (we use a Runge–Kutta scheme).

$$\nabla\cdot\mathbf{u}=0 \tag{1a}$$

$$\frac{\partial\rho\mathbf{u}}{\partial t}+\nabla\cdot(\rho\mathbf{u}\otimes\mathbf{u})=-\nabla p+\rho\mathbf{g}+\sigma\kappa\mathbf{n}\delta_\sigma+\nabla\cdot(\mu(\nabla\mathbf{u}+\nabla^T\mathbf{u})) \tag{1b}$$

$$\frac{\partial\chi_k}{\partial t}=-\mathbf{u}\cdot\nabla\chi_k \tag{1c}$$

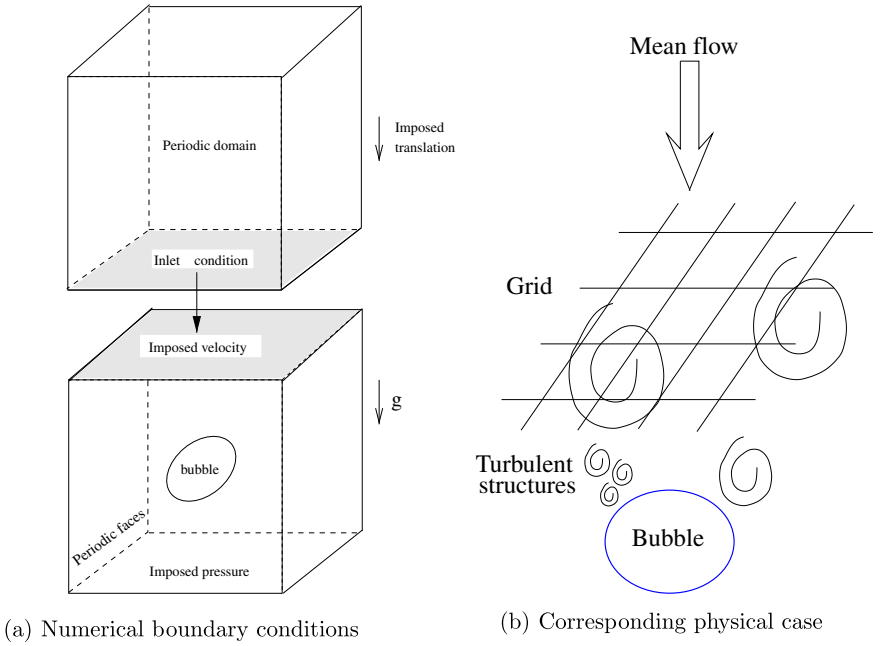

(a) Numerical boundary conditions (b) Corresponding physical case

Fig. 1. Interaction of a buoyant deformable bubble with a spatially decaying turbulence.

with

$$\nabla\chi_k = -\mathbf{n}_k\delta_\sigma \tag{2}$$

where t is the time, $\mathbf{u}$ the velocity, p the pressure, ρ the density, μ the dynamic viscosity, $\mathbf{n} = \mathbf{n}_g$ the normal to the interface (from gas to liquid), κ the interface curvature and δ_σ the Dirac function indicating the interface. The system (1) is valid on the entire domain in the sense of distributions (see, e.g., Kataoka, 1986). The numerical method is described in previous works (Calvin et al., 2002; Mathieu, 2003, 2004; Labourasse et al., 2007).

2.2. Boundary conditions and validation tests

To perform the DNS of a deformable bubble in a decaying turbulence, two computations are realized. The first one, simulation s_1, is a single-phase flow, that corresponds to the classical homogeneous isotropic turbulence in a three-dimensional periodic box. The second one, simulation s_2, is a two-phase simulation. First, each simulation reaches separately a statistically steady state. Then, a uniform translation motion is added in order to perform the simulation in the bubble's frame of reference. Finally, we use one boundary of s_1 as an inlet condition of imposed velocity for the simulation s_2 (see Figs. 1 and 2). Doing this coupling, the simulation mimics the physical situation of a buoyant bubble rising against a downwards flow passing through a fixed grid. The grid creates a decaying turbulence that interacts with the downstream bubble. The mesh size of the simulations s_1 and s_2 is $128 \times 128 \times 128$ allocated to 8 processors. We have paid a particular attention to the task of providing realistic inlet conditions that reproduces the velocity field of a grid turbulence. Indeed, in s_1, kinetic energy is rescaled at every time step. Our method to force turbulence corresponds to a linear forcing method proposed by Lundgren (2003). Our results are in agreement which those of Rosales and Meneveau (2005). In particular, we find the Kolmogorov $k^{-\frac{5}{3}}$ slope and the most energetic structures (that correspond also to the beginning of the inertial zone) have the size of the domain of simulation (Fig. 3). Furthermore, we evaluate the Kolmogorov length scale thanks to the dissipation rate that we would have without a forcing method. We found $\eta = 2.1 \times 10^{-4}$ m whereas the mesh size is 9.8×10^{-5} m. Thus, s_1 is fully resolved (i.e. the mesh size is fine

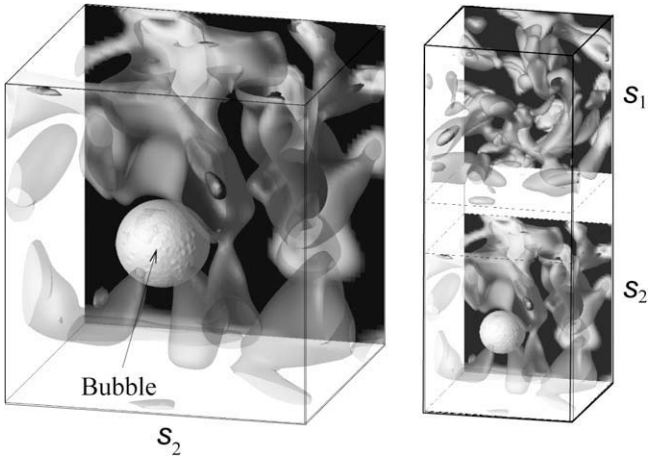

Fig. 2. Visualization of bubble and Q-isosurfaces.

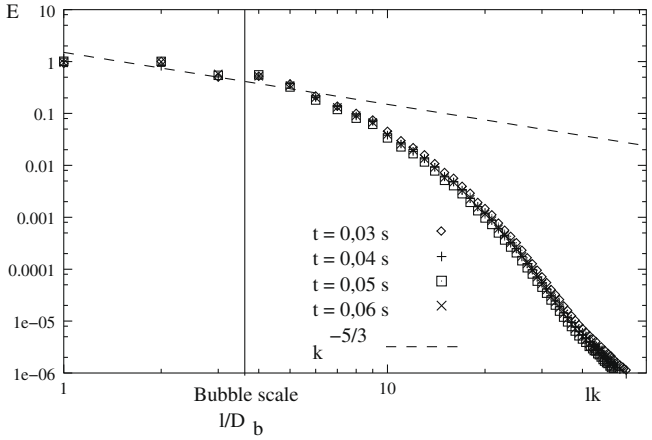

Fig. 3. Kinetic energy spectrum (l domain length).

Table 1
Dimensionless numbers. In this table, we use the following definitions, $Re_b = \frac{V_T D_b}{\nu_l}$, $We = \frac{\rho_l e_c D_b}{\sigma}$, $Mo = \frac{g\mu_l^4}{\rho_l \sigma^3}$ and $Bo = \frac{\rho_l g D_b^2}{\sigma}$ where V_T is the terminal velocity of the bubble in the laminar case, D_b the bubble diameter, ν_l the kinematic viscosity of the liquid and e_c the kinetic energy density of the simulation s_1.

Re_b	We	Mo	Bo	$\frac{\eta}{D_b}$	$\frac{L}{D_b}$	$\frac{T}{T_b}$
25.8	0.2	2.2×10^{-5}	2.1	0.06	1.4	0.5

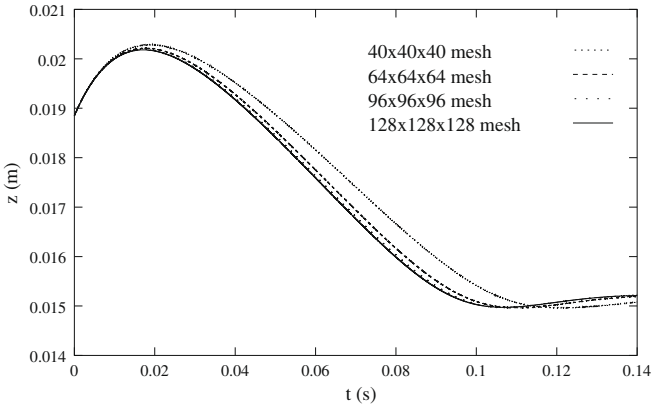

Fig. 4. Mesh convergence for the laminar case of a single rising bubble (s_2): time evolution of the vertical coordinate of the bubble's center of gravity.

enough to capture the smallest coherent turbulent structures). In s_2, we simulate the interaction of the buoyant bubble with the spatially decaying turbulence. The size of our bubble is in the inertial zone of the kinetic energy spectrum (see Fig. 3). The most relevant dimensionless numbers of the simulation are given in Table 1 (η is the Kolmogorov length scale, D_b the bubble diameter, T_b the relaxation time of the bubble, T and L the time and space integral scales, respectively). Finally, we realize a mesh convergence for the laminar case of a simple rising bubble. We demonstrate that a $96 \times 96 \times 96$ mesh is enough to capture the terminal velocity of the bubble (i.e. the mesh size is fine enough to capture the bubble dynamic, see Fig. 4). Because the smallest turbulence scales are generated by $s1$ and because the smallest scales related to the two-phase flow correspond to the laminar boundary layer at the bubble surface, the fact that the mesh size is fine enough to capture the flow for $s1$ and $s2$ without coupling implies that the mesh size is fine enough to capture the flow resulting from the coupling of $s1$ and $s2$. More details about this DNS could be found in Toutant et al. (2008).

3. Velocity of the under-resolved discontinuous interface

In this section, we evaluate the potential of the ISS model to estimate the velocity of the under-resolved discontinuous interface. We note this velocity $v_{\tilde{\sigma}}$:

$$\frac{\partial \tilde{\chi}_g}{\partial t} = v_{\tilde{\sigma}} \delta_{\tilde{\sigma}} \tag{3}$$

The ISS model of this velocity is noted $v_{\tilde{\sigma}}^m$. In order to evaluate the ISS model, it is necessary to calculate *with the DNS data* $v_{\tilde{\sigma}}^m$ and $v_{\tilde{\sigma}}$. These calculations are explained in Sections 3.1 and 3.2, respectively. In Section 3.3, the model is interpreted as a deconvolution of the surface filtering operation. The explicit calculation of the surface filtering operation is explained in Section 3.4. Finally in Section 3.5, the results in terms of difference between the model velocity $v_{\tilde{\sigma}}^m$ and the real velocity $v_{\tilde{\sigma}}$ are analysed.

3.1. Evaluation of the modeling expression with DNS data

In part 1, we have determined the transport equation of the phase indicator function in the ISS modeling case:

$$v_{\tilde{\sigma}}^m = \tilde{\mathbf{u}} \cdot \tilde{\mathbf{n}} + \left(\widetilde{\tilde{\mathbf{u}} \cdot \tilde{\mathbf{n}}^\sigma} - \widetilde{\tilde{\mathbf{u}}^\sigma} \cdot \widetilde{\tilde{\mathbf{n}}^\sigma} \right) + \frac{r^2}{10} \left(\Delta_s(\mathbf{v}_{\tilde{\sigma}}^m) \cdot \tilde{\mathbf{n}} + 2 \nabla_s(\mathbf{v}_{\tilde{\sigma}}^m) : \nabla_s(\tilde{\mathbf{n}}) \right) \tag{4}$$

This equation gives the ISS model of the velocity of the under-resolved discontinuous interface $v_{\tilde{\sigma}}^m$ as a function of the known velocity $\tilde{\mathbf{u}}$ and of the known normal $\tilde{\mathbf{n}}$.

In order to evaluate the velocity given by the ISS model $v_{\tilde{\sigma}}^m$, the velocity and the normal of the ISS description level, $\tilde{\mathbf{u}}$ and $\tilde{\mathbf{n}}$, are required. The DNS only gives the velocity $\mathbf{u}$ and the normal $\mathbf{n}$. The velocity and the normal of the ISS description level, $\tilde{\mathbf{u}}$ and $\tilde{\mathbf{n}}$, have to be calculated. Because the operator $\tilde{\cdot}$ is the asymptotic limit of the operator $\bar{\cdot}$, we do not have an explicit equation that defines $\tilde{\cdot}$ and this operator has to be estimated. Actually, we only need to estimate the effect of this operator on the velocity and on the normal at the interface.

Regarding the velocity, by definition of the ISS description level (see part 1 Toutant et al., accepted for publication), we have in the entire domain:

$$\tilde{\mathbf{u}} = \bar{\mathbf{u}}^{\mathbf{0}} \tag{5}$$

We want to show that, at order zero and at the interface, one gets:

$$\tilde{\mathbf{u}}|_{\xi_3^0=0} = \bar{\mathbf{u}}^\sigma \tag{6}$$

By definition of the surface filtering operation (see part 1 Eq. (48)), we have:

$$\bar{\mathbf{u}}^\sigma(\xi_1^0, \xi_2^0) = \int_{\mathbb{R}^2} G_\sigma(\xi_1^0 - \xi_1, \xi_2^0 - \xi_2) \mathbf{u}(\xi_1, \xi_2, \xi_3 = 0) d\xi_1 d\xi_2 \tag{7}$$

By definition of the volume filtering operation (see part 1 Eq. (4a) and part 1 Section 4.2.5 for the decomposition of the three-dimensional kernel G), we have:

$$\bar{\mathbf{u}}(\xi_1^0, \xi_2^0, \xi_3^0 = 0) = \int_{\mathbb{R}^3} G_\sigma(\xi_1^0 - \xi_1, \xi_2^0 - \xi_2) G_3(\xi_3^0 - \xi_3) \times \mathbf{u}(\xi_1, \xi_2, \xi_3) d\xi_1 d\xi_2 d\xi_3 \tag{8}$$

Since the velocity $\mathbf{u}$ is continuous at the interface ($\xi_3^0 = 0$) at the DNS scale, we can perform the following Taylor expansion around $\xi_3^0 = 0$:

$$\begin{aligned} \mathbf{u}(\xi_1, \xi_2, \xi_3) &= \mathbf{u}(\xi_1, \xi_2, \xi_3^0 = 0) + \mathcal{O}(\xi_3 - \xi_3^0) \\ &= \mathbf{u}(\xi_1, \xi_2, \xi_3^0 = 0) + \mathcal{O}(\epsilon) \end{aligned} \tag{9}$$

Injecting this expression in Eq. (8), one gets:

$$\bar{\mathbf{u}}(\xi_1^0, \xi_2^0, \xi_3^0 = 0) = \int_{\mathbb{R}^3} G_\sigma(\xi_1^0 - \xi_1, \xi_2^0 - \xi_2) G_3(\xi_3^0 - \xi_3) \times \mathbf{u}(\xi_1, \xi_2, \xi_3^0 = 0) d\xi_1 d\xi_2 d\xi_3 + \mathcal{O}(\epsilon) \tag{10}$$

By definition, we have $\bar{\mathbf{u}} = \bar{\mathbf{u}}^0 + \mathcal{O}(\epsilon)$ (see part 1 Eq. (23)). Thus, by identification and using the property of the normal part G_3 of the three-dimensional kernel, one gets:

$$\bar{\mathbf{u}}^0(\xi_1^0, \xi_2^0, \xi_3^0 = 0) = \int_{\mathbb{R}^2} G_\sigma(\xi_1^0 - \xi_1, \xi_2^0 - \xi_2) \times \mathbf{u}(\xi_1, \xi_2, \xi_3^0 = 0) d\xi_1 d\xi_2 = \bar{\mathbf{u}}^\sigma(\xi_1^0, \xi_2^0) \tag{11}$$

Regarding the normal, one can prove that the local mass conservation imposed in part 1. (See Eq. (55) of part 1.) implies that the normal of the equivalent interface, $\tilde{\mathbf{n}}$, is equal at order zero to the filtered normal of the exact interface, $\bar{\mathbf{n}}^\sigma$. The demonstration is given in Appendix A.

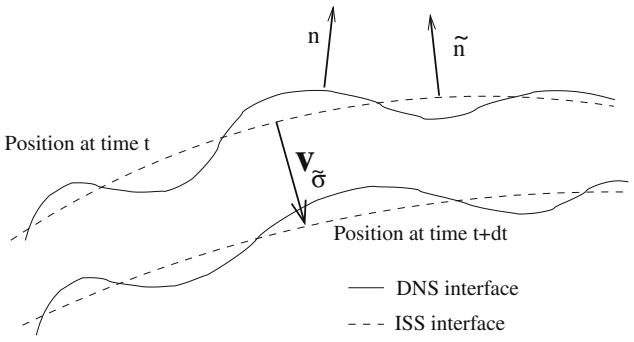

Fig. 5. Definition of the reference velocity of the ISS interface motion.

Therefore, the velocity of the ISS model is well approximated by:

$$v_{\bar{\sigma}}^{m} = \bar{\mathbf{u}}^{\sigma}\cdot\bar{\mathbf{n}}^{\sigma} + \left(\overline{\bar{\mathbf{u}}^{\sigma}\cdot\bar{\mathbf{n}}^{\sigma}}^{\sigma} - \overline{\bar{\mathbf{u}}^{\sigma}}^{\sigma}\cdot\overline{\bar{\mathbf{n}}^{\sigma}}^{\sigma}\right) + \frac{r^2}{10}\left(\Delta_s(\mathbf{v}_{\bar{\sigma}}^{m})\cdot\bar{\mathbf{n}}^{\sigma} + 2\nabla_s(\mathbf{v}_{\bar{\sigma}}^{m}) : \nabla_s(\bar{\mathbf{n}}^{\sigma})\right) \quad (12)$$

3.2. Reference velocity

The reference velocity $v_{\tilde{\sigma}}$ is the exact velocity of the under-resolved discontinuous interface that we have to compare to the velocity given by the ISS model $v_{\bar{\sigma}}^{m}$. The most precise way to calculate the reference velocity is the following algorithm:

- store the DNS interface geometry at each time step χ^t,
- apply a volume filter to this interface to obtain the continuous transition zone $\bar{\chi}^t$,
- reconstruct a discontinuous interface that corresponds to the ISS interface $\bar{\chi}^t$ and
- evaluate the motion of the ISS interface during each time step.

This algorithm is very complex to implement and requires too much data storage. To simplify this algorithm, we assume that the geometry of the under-resolved discontinuous interface is well described using the surface filtering operation, $\bar{\mathbf{n}}^{\sigma}$. This assumption is equivalent to use $\tilde{\mathbf{n}} = \bar{\mathbf{n}}^{\sigma}$. In Appendix A, we prove that this equality is true at order zero. Consequently, we pass from the DNS interface to the ISS interface applying the surface filtering operation. Furthermore, by definition the DNS interface location at time t is moved to its location at time $t+\delta t$ by the DNS velocity field, $\mathbf{u}$. Thus, the velocity of the ISS interface $v_{\tilde{\sigma}}$ is well approximated by (Fig. 5):

$$v_{\tilde{\sigma}} = \mathbf{u}\cdot\bar{\mathbf{n}}^{\sigma} \quad (13)$$

3.3. Interpretation of the model

The proposed model is good if the modeled velocity is a good approximation of the real velocity $v_{\bar{\sigma}}^{m} \approx v_{\tilde{\sigma}}$ or, it is equivalent, if the difference between the velocity of the microscopic level $\mathbf{u}\cdot\bar{\mathbf{n}}^{\sigma}$ and the velocity of the macroscopic level $\bar{\mathbf{u}}^{\sigma}\cdot\bar{\mathbf{n}}^{\sigma}$ is well approximated by the scale similarity hypothesis and the time evolution of the curvature. One notes τ_{disc} the difference between the velocity and τ_{disc}^{m} the corresponding model:

$$\tau_{disc} = \mathbf{u}\cdot\bar{\mathbf{n}}^{\sigma} - \bar{\mathbf{u}}^{\sigma}\cdot\bar{\mathbf{n}}^{\sigma} = (\mathbf{u}-\bar{\mathbf{u}}^{\sigma})\cdot\bar{\mathbf{n}}^{\sigma} \quad (14a)$$

$$\tau_{disc}^{m} = \left(\overline{\bar{\mathbf{u}}^{\sigma}\cdot\bar{\mathbf{n}}^{\sigma}}^{\sigma} - \overline{\bar{\mathbf{u}}^{\sigma}}^{\sigma}\cdot\overline{\bar{\mathbf{n}}^{\sigma}}^{\sigma}\right) + \frac{r^2}{10}\left(\Delta_s(\mathbf{v}_{\bar{\sigma}}^{m})\cdot\bar{\mathbf{n}}^{\sigma} + 2\nabla_s(\mathbf{v}_{\bar{\sigma}}^{m}) : \nabla_s(\bar{\mathbf{n}}^{\sigma})\right) \quad (14b)$$

The model is good if $\tau_{disc}^{m} \approx \tau_{disc}$. The previous definition of τ_{disc} shows that the model has to reconstruct the normal velocity $\mathbf{u}\cdot\bar{\mathbf{n}}^{\sigma}$ thanks to the velocity filtered by the surface filtering operation $\bar{\mathbf{u}}^{\sigma}\cdot\bar{\mathbf{n}}^{\sigma}$. So, the model τ_{disc}^{m} is good if it enables the deconvolution of the surface filtering operation $\bar{\cdot}^{\sigma}$. It is worth noting that there is a surface Laplacian in the expression of τ_{disc}^{m}. In the single-phase LES modeling case, the velocity fluctuations are estimated by the Laplacian of the mean velocity when one uses deconvolution methods (Sagaut, 2003). Thanks to the matched expansion methods, we see that the Laplacian is also a part of the model for the deconvolution of a surface filter. Physically, the term that is due to the curvature time evolution and that involves the Laplacian $\frac{r^2}{10}(\Delta_s(\mathbf{v}_{\bar{\sigma}}^{m})\cdot\bar{\mathbf{n}}^{\sigma} + 2\nabla_s(\mathbf{v}_{\bar{\sigma}}^{m}) : \nabla_s(\bar{\mathbf{n}}^{\sigma}))$ corresponds to the effects of the subgrid velocity fluctuations on the bubble geometry.

3.4. Discrete filtering surface operations

In this section, we describe how the surface filtering operation is explicitly calculated. At the DNS scale, the interface is explicitly described by a Lagrangian mesh moving on an Eulerian mesh. This Lagrangian mesh is constituted by markers. In each marker i of the Lagrangian mesh and for a given variable ϕ defined on the interface the resulting filtered field $\bar{\phi}_i^{\sigma}$ is computed recursively as follows

$$\hat{\phi}_i = \frac{1}{N_i+1}\left(\phi_i + \sum_{j\in E_i}\phi_j\right) \quad (15a)$$

$$\hat{\hat{\phi}}_i = \frac{1}{N_i+1}\left(\hat{\phi}_i + \sum_{j\in E_i}\hat{\phi}_j\right) \quad (15b)$$

$$\bar{\phi}_i^{\sigma} = \hat{\hat{\hat{\phi}}}_i = \frac{1}{N_i+1}\left(\hat{\hat{\phi}}_i + \sum_{j\in E_i}\hat{\hat{\phi}}_j\right) \quad (15c)$$

where E_i is the set of the closest neighbors of i and N_i is the number of the closest neighbors of i. Fig. 6 shows the principle of this recursive filter. We choose to apply the filter three times because it corresponds to the largest filter size that is allowed by the assumption of the ISS model.[2]

This explicit recursive filter does not correspond to the theoretical filter we use to develop the ISS model.[3] Indeed, we use a spherical filter to find the closure relation for the time evolution of the filtered phase indicator (Section 4.3.2.2 of part 1). To take into account this difference (that will ever exist in a practical way because the implicit filtering operation is unknown), we introduce the coefficients c_0 and c_1 in the ISS model:

$$v_{\bar{\sigma}}^{m} = \bar{\mathbf{u}}^{\sigma}\cdot\bar{\mathbf{n}}^{\sigma} + c_0\left(\overline{\bar{\mathbf{u}}^{\sigma}\cdot\bar{\mathbf{n}}^{\sigma}}^{\sigma} - \overline{\bar{\mathbf{u}}^{\sigma}}^{\sigma}\cdot\overline{\bar{\mathbf{n}}^{\sigma}}^{\sigma}\right) + c_1\frac{r^2}{10}\left(\Delta_s(\mathbf{v}_{\bar{\sigma}}^{m})\cdot\bar{\mathbf{n}}^{\sigma} + 2\nabla_s(\mathbf{v}_{\bar{\sigma}}^{m}) : \nabla_s(\bar{\mathbf{n}}^{\sigma})\right) \quad (16)$$

These coefficients c_0 and c_1 are the parameters of our model to take into account the difference between the theoretical filtering operation and the numerical one. We determine these parameters by minimizing the difference between the modeled velocity $\mathbf{v}_{\bar{\sigma}}^{m}$ and the real velocity $\mathbf{v}_{\tilde{\sigma}}$ of the under-resolved discontinuous interface.

In the previous equation, the modeled velocity is defined in function of itself: it is an implicit definition. This implicit definition of the velocity of the under-resolved discontinuous interface implies that it is varying non-linearly as a function of the coefficients c_0 and c_1. In order to determine these parameters we use the simplex algorithm (Nelder and Mead, 1965). Thanks to this algorithm, we minimize the integral error over a relevant time. At each time step, the error is

[2] The curvature is supposed to evolve slowly in the filter control volume.

[3] Actually, the ISS model is essentially developed without choosing a particular filter. However, the term related to the time evolution of the curvature requires to choose a particular filter (see Eq. (60) part 1).

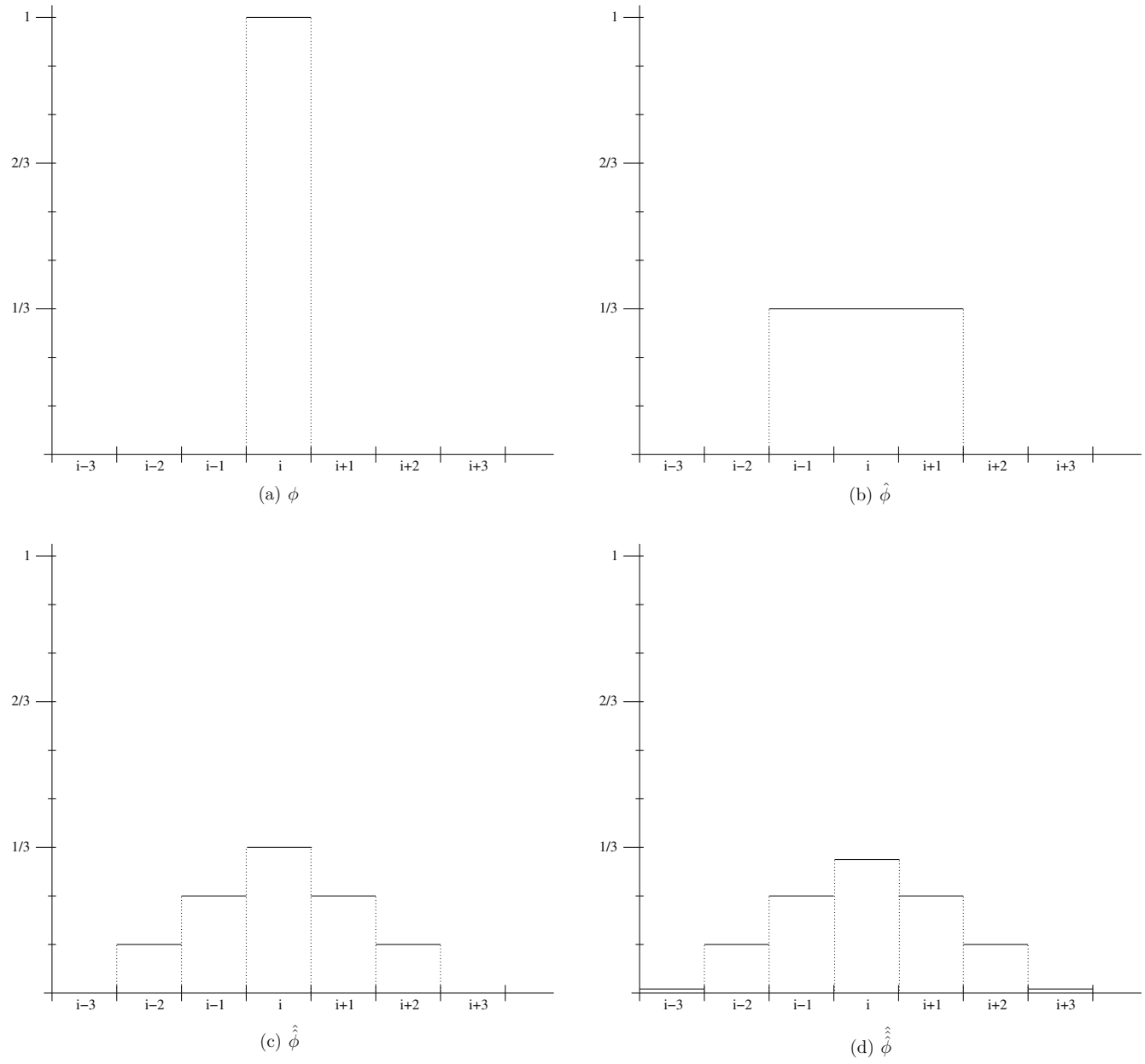

Fig. 6. Definition of the filtered fields.

$$E = \frac{\sum_{k=1}^{N} \left(\tau_{disc}(\mathbf{x}_k) - \tau_{disc}^{m}(\mathbf{x}_k)\right)^2}{\sum_{k=1}^{N} \left(\tau_{disc}(\mathbf{x}_k)\right)^2} \tag{17}$$

where N is the number of Lagrangian points describing the interface and $\mathbf{x}_k$ the coordinates of the point k. We integrate the error E over the time for each tested couple $(c_0; c_1)$. The minimum is found for $(c_0 = 1.5, c_1 = 0.36)$. The mean error is then 8%. All the results described in the next section are obtained with these parameters.

3.5. Results

Fig. 7 shows the time evolution of the error E (Eq. (17)) when the term τ_{disc} is modeled:

- only by the surface similarity scale hypothesis $c_0(\overline{\overline{\mathbf{u}}^{\sigma} \cdot \overline{\mathbf{n}}^{\sigma}}^{\sigma} - \overline{\overline{\mathbf{u}}^{\sigma}}^{\sigma} \cdot \overline{\overline{\mathbf{n}}^{\sigma}}^{\sigma})$ $(c_0 = 1.5)$,
- only by taking into account the time evolution of the curvature $c_1 \frac{r^2}{10}(\Delta_s(\mathbf{v}_{\sigma}^{m}) \cdot \bar{\mathbf{n}}^{\sigma} + 2\nabla_s(\mathbf{v}_{\sigma}^{m}) : \nabla_s(\bar{\mathbf{n}}^{\sigma}))$ $(c_1 = 0.36)$ and
- by the whole model τ_{disc}^{m} that uses the last two terms.

The comparison is performed over more than 500 time steps. The averaged error in time (more than 500 time steps) and space (bubble surface) is smaller than 10%. Because ISS modeling is local and because a lot of turbulent structures of very different scales interact with small parts of the interface, one time step is already a very complete test case and the average over more than 500 time steps could be considered as a statistical error. This is confirmed by the fact that increasing the tested interval does not change the averaged error. Fig. 7 shows that 50% of the subgrid term is modeled by only one of the two contributions of the proposed model. Using both the term related to the scale similarity hypothesis and the term related to the time evolution of the curvature (the whole model), more than 90% is correctly modeled. If the parameters $(c_0; c_1)$ are optimized separately, similar results are obtained. Consequently, the two terms are required to correct the displacement of the equivalent discontinuity. Furthermore, we note that their behaviors are quite different and they seem to be complementary. Indeed, a local maximum of the error using the scale similarity corresponds to a local minimum of the error using the time

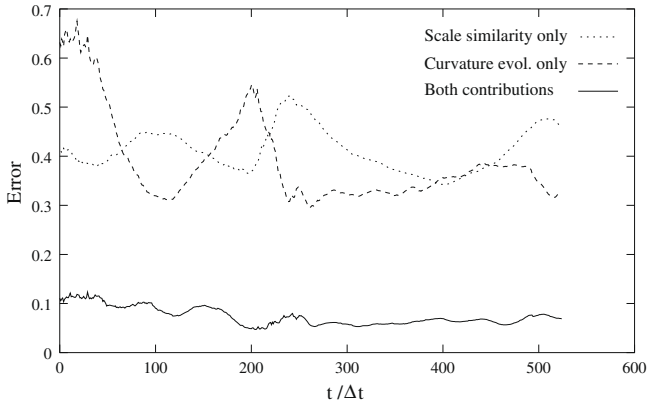

Fig. 7. Time evolution of the interface transport error. In the case of a model: with only the similarity scale, with only the time evolution of the curvature, combining the two terms.

evolution of the curvature (and *vice-versa*). In this way, although the error of one contribution of the model is strongly varying, the error of the whole model is almost constant. At $t = 200\Delta t$ for example, the term related to the time evolution of the curvature is much more useful than the term related to the scale similarity. At $t = 500\Delta t$, it is the contrary. It is not surprising that the term related to the time evolution of the curvature models up to more than 60% of the subgrid term because it depends on the Laplacian of the velocity that is a good approximation of velocity fluctuations.

In order to better understand the role of each contribution, Figs. 8–10 show them on the interface at time $t = 0, t = 200\Delta t$ and $t = 500\Delta t$ (respectively). These three times correspond to the three kind of complementarities of the terms. For $t = 500\Delta t$ (Fig. 10), the patterns are the same but the intensity of the terms are different. For $t = 0$ (Fig. 8), the patterns are almost the same but the locations where their sign shifts are clearly distinct. For $t = 200\Delta t$ (Fig. 9), the two terms do not have the same patterns. In any case, only the sum of the two terms (Figs. 8–10(b)) allows to correctly estimate both the pattern and the intensity of the subgrid term (Figs. 8–10(b)). Consequently, the error (Figs. 8–10(e)) represents less than 10% of the subgrid term. This statement is corroborated by the correlations of each term and the whole model with the real contribution (Figs. 11–13). The whole model is very well correlated to the real contribution (Figs. 11–13(a)). At the beginning of the simulation (Fig. 11), the model is a little less efficient. It is due to the large curvatures of the interface that are a limit of validity of our model. The correlations of the isolated terms are not as good (Figs. 11–13(b) and Figs. 11–13(c)): the dispersion of isolated

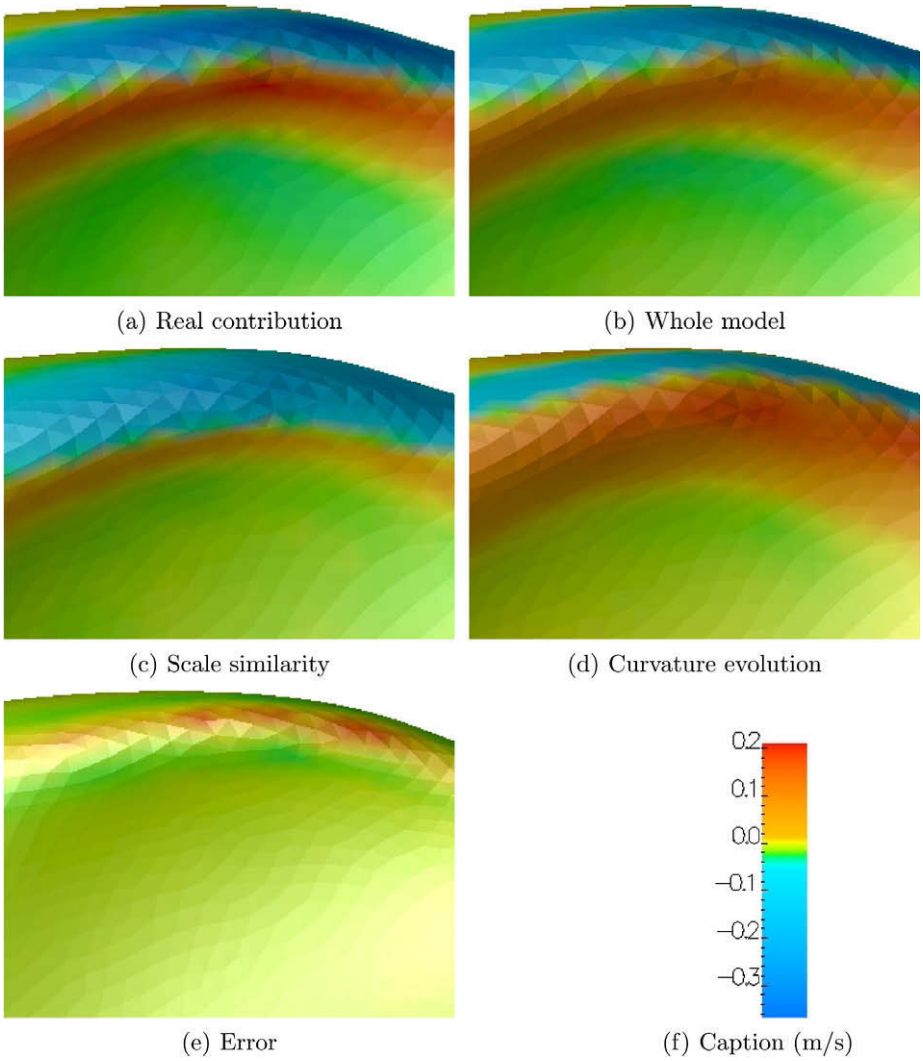

Fig. 8. Comparison between the proposed models and the real contribution, $t = 0$.

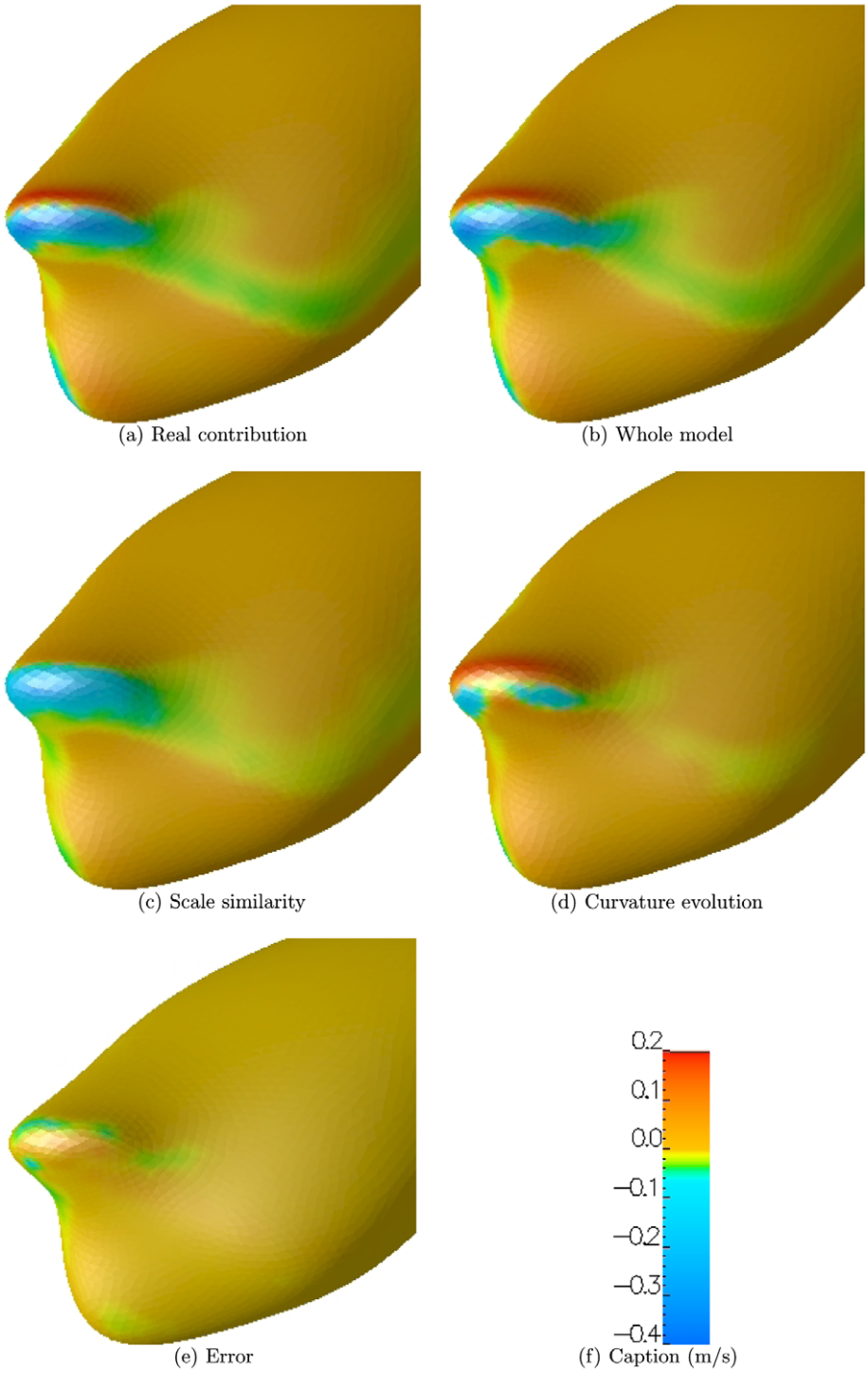

Fig. 9. Comparison between the proposed models and the real contribution, $\frac{t}{\Delta t} = 200$.

terms is much more important. We note again their complementarities: although the scale similarity underestimates the subgrid term, the time evolution of the curvature overestimates it. Thus, both the interest of the proposed model and the complementarities of the two terms are confirmed.

4. Conclusions and perspectives

We use a simulation that is representative of the interactions between interfaces and turbulence. This simulation is relevant to evaluate the ISS model because the Kolmogorov length scale is much smaller than the bubble diameter and the interface is strongly deformed by the turbulent structures. Due to the impossibility to define *a priori* the ISS variables, we only test the interface transport equation of the ISS model (the momentum jump conditions are not tested). However, we think that it is more important to test the interface transport equation than the momentum jump conditions. Indeed, the closure of the under-resolved discontinuous interface transport equation requires more modeling assumptions than the closure of the momentum equation. The *a priori* tests

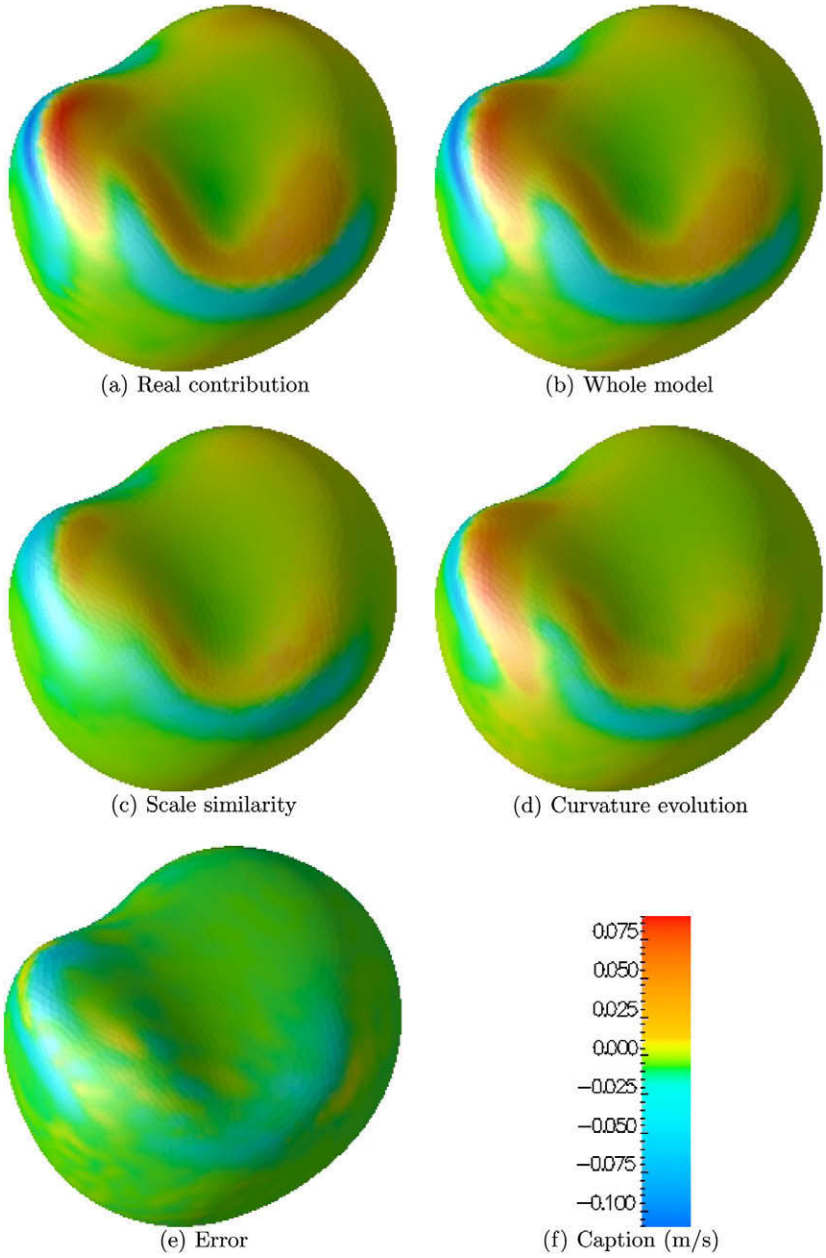

Fig. 10. Comparison between the proposed models and the real contribution, $\frac{t}{\Delta t} = 500$.

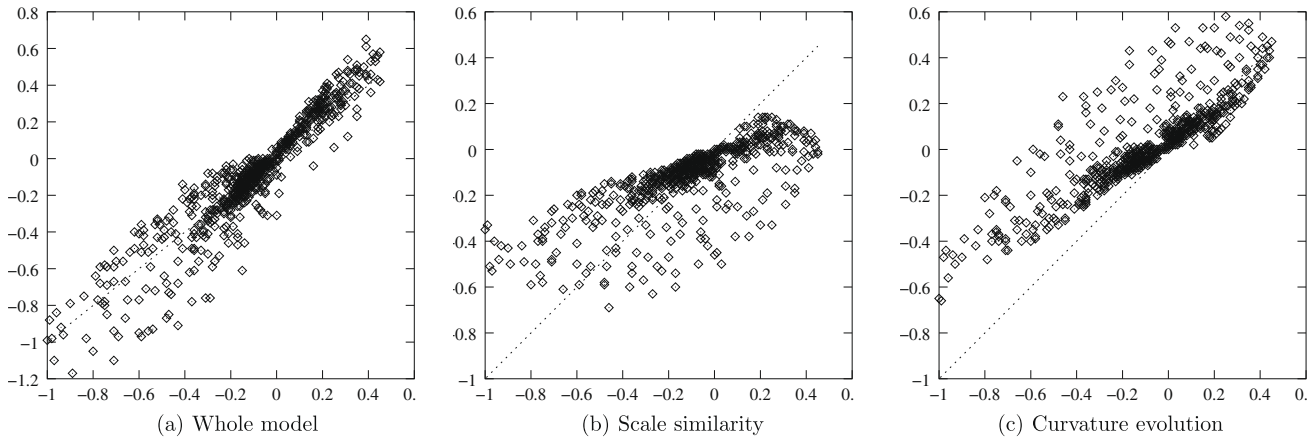

Fig. 11. Correlation between the model and the real contribution of the subgrid term of the interface transport equation, $t = 0$.

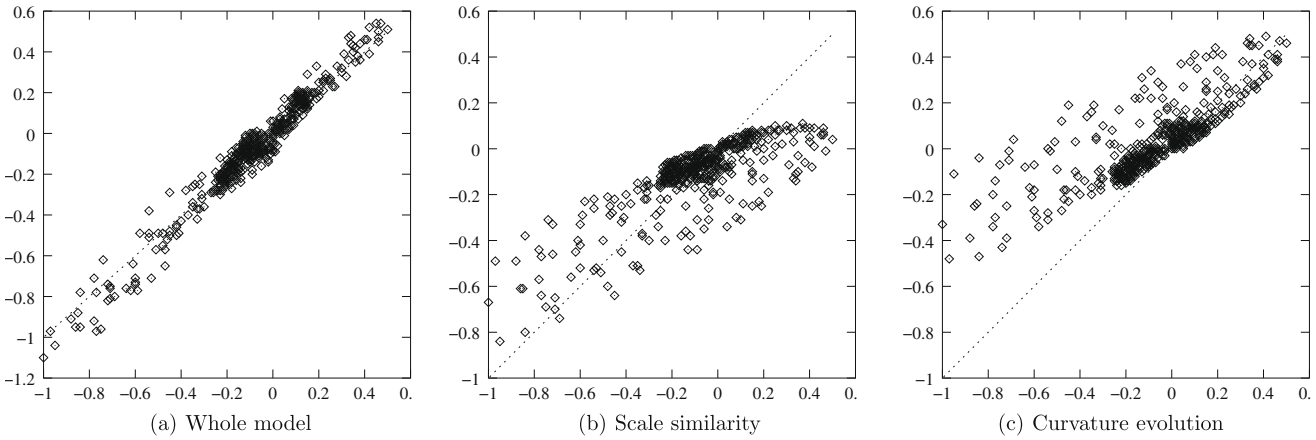

Fig. 12. Correlation between the model and the real contribution of the subgrid term of the interface transport equation, $\frac{t}{\Delta t} = 200$.

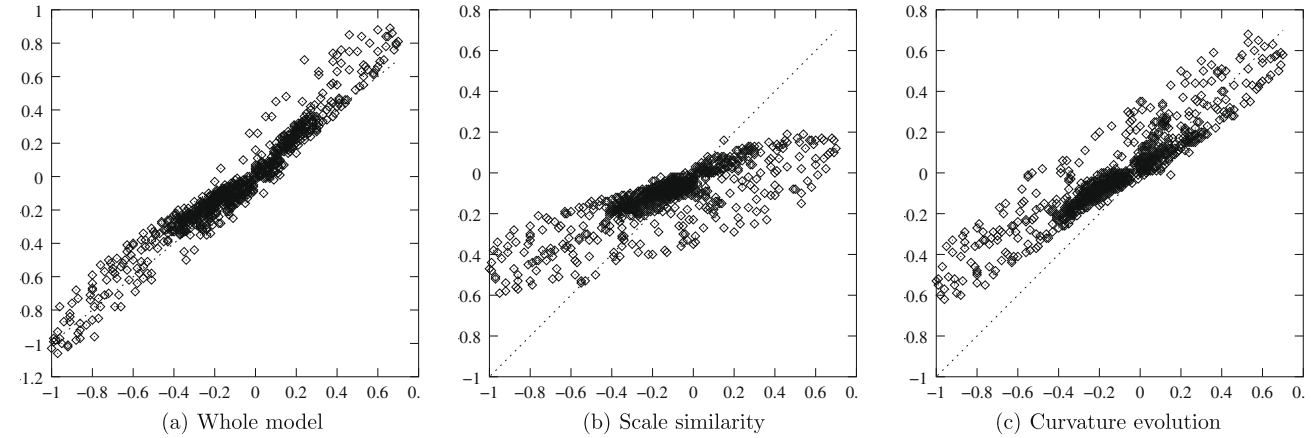

Fig. 13. Correlation between the model and the real contribution of the subgrid term of the interface transport equation, $\frac{t}{\Delta t} = 500$.

realized with the DNS data prove that a surface scale similarity hypothesis and the time evolution of the curvature precisely correct the velocity of the equivalent interface. These two terms appear to be complementary:

- the term related to the surface scale similarity hypothesis takes into account the correlations between the normal at the interface and the velocity of the phases,
- the term related to the time evolution of the curvature takes into account the effect of the subgrid velocity fluctuations on the interface geometry.

We have now implemented the ISS models. We are currently realizing *a posteriori* tests in order to evaluate the gain (in terms of numerical costs) that ISS allows compared to DNS.

Appendix A. Normal of the equivalent interface and filtered normal of the exact interface

In this section, we prove that the local mass conservation (Eq. (55) of part 1) imposed in Section 4.3.1 of part 1 implies that the normal of the equivalent interface, $\tilde{\mathbf{n}}$, is equal at order zero to the filtered normal of the exact interface, $\bar{\mathbf{n}}^{\sigma}$. Taking the gradient of the local mass conservation (Eq. (55)) one finds at order zero:

$$0 = \int_V \left(\nabla\tilde{\chi}_g - \overline{\nabla\chi_g}\right) dV \tag{A.1a}$$

$$= \int_V \left(-\tilde{\mathbf{n}}\delta_{\tilde{\sigma}} - \overline{\nabla\chi_g}\right) dV \tag{A.1b}$$

$$= \int_V \left(-\tilde{\mathbf{n}}\delta_{\tilde{\sigma}} - \overline{\mathbf{n}\chi_{g,3}}\right) dV \tag{A.1c}$$

$$= \int_V (\bar{\mathbf{n}}^{\sigma} G_3(\xi_3) - \tilde{\mathbf{n}}\delta_{\tilde{\sigma}}) dV \tag{A.1d}$$

At order zero, an integral over V could be reduced to an integral over the direction normal to the interface (see Eq. (B.6) of part 1). Thus, the previous equation gives:

$$\int (\bar{\mathbf{n}}^{\sigma} G_3(\xi_3) - \tilde{\mathbf{n}}\delta_{\tilde{\sigma}}) d\xi_3 = 0 \tag{A.2}$$

Finally, we obtain:

$$\tilde{\mathbf{n}} = \bar{\mathbf{n}}^{\sigma} \tag{A.3}$$

References

Bunner, B., Tryggvason, G., 2003. Effect on bubble deformation on the properties of bubbly flows. J. Fluid Mech. 495, 77–118.
Calvin, C., Cueto, O., Emonot, P., 2002. An object-oriented approach to the design of fluid mechanics software. Math. Model. Numer. Anal. 36, 907–921.

Février, P., Simonin, O., Squires, K., 2005. Partitioning of particle velocities in gas–solid turbulent flows into a continuous field and a spatially uncorrelated random distribution: theoretical formalism and numerical study. J. Fluid Mech. 533, 1–46.

Kataoka, I., 1986. Local instant formulation of two-phase flow. Int. J. Multiphase Flow 12, 745–758.

Labourasse, E., Lacanette, D., Toutant, A., Lubin, P., Vincent, S., Lebaigue, O., Caltagirone, J.P., Sagaut, P., 2007. Towards large eddy simulation of isothermal two-phase flows: governing equations and a priori tests. Int. J. Multiphase Flow 33, 1–39.

Lu, J., Fernandez, A., Tryggvason, G., 2005. The effects of bubbles on the wall shear in a turbulent channel flow. Phys. Fluids 17 (12 pp.).

Lundgren, T., 2003. Linearly forced isotropic turbulence. In: Annual Research Briefs. Center for Turbulence Research, Stanford, pp. 461–473.

Mathieu, B., 2003. Etude physique, expérimentale et numérique des mécanismes de base intervenant dans les écoulements diphasiques, Ph.D. thesis, University of Provence.

Mathieu, B., Demonstration of a 3d parallel implementation of the front-tracking method: simulation of fluid mixing with a moving boundary and a free surface. In: Proceedings of Advances in the Modeling Methodologies of Two-Phase Flows Meeting. Lyon, France, 24–26 November, 2004.

Merle, A., Legendre, D., Magnaudet, J., 2005. Forces on a high-Reynolds-number spherical bubble in a turbulent flow. J. Fluid Mech. 532, 53–62.

Nelder, J.A., Mead, R., 1965. A simplex for function minimization. Comput. J. 7, 308–313.

Rosales, C., Meneveau, C., 2005. Linear forcing in numerical simulations of isotropic turbulence: physical space implementations and convergence properties. Phys. Fluids 17, 509–529.

Sagaut, P., 2003. Large Eddy Simulation for Incompressible Flows. Springer Verlag.

Toutant, A., Chandesris, M., Jamet, D., Lebaigue, O., accepted for publication. Jump conditions for filtered quantities at an under-resolved discontinuous interface Part 1: theoretical development. Companion paper. Int. J. Multiphase Flow.

Toutant, A., Labourasse, E., Lebaigue, O., Simonin, O., 2008. DNS of the interaction between a deformable buoyant bubble and a spatially decaying turbulence: a priori tests for LES two-phase flow modelling. Comput. Fluids 37, 877–886.